Synthesis, Structure, and Properties of Azatriangulenium Salts

Bo W. Laursen* and Frederik C. Krebs[a]

Abstract: A general synthetic route to novel nitrogen-bridged heterocyclic carbenium ions of the acridinium and triangulenium type has been developed and investigated. The synthetic method is based on nucleophilic aromatic substitution (S_NAr) on the tris(2,6-dimethoxyphenyl)carbenium ion (**1**) with primary amines and, by virtue of its stepwise and irreversible nature, provides a powerful tool for the preparation of a wide variety of new heterocyclic carbenium salts. Several derivatives of the three new oxygen- and/or nitrogen-bridged triangulenium salts, azadioxa- (**6**), diazaoxa- (**7**), and triazatriangulenium (**4**), have been synthesized and their physicochemical properties have been investigated. Crystal structures for compounds **2b-PF$_6$**, **2d-PF$_6$**, **4b-BF$_4$**, **4c-BF$_4$**, **6e-BF$_4$**, and **8** are reported. The different packing modes found for the triazatriagulenium salts are discussed in relation to the electrostatic and space-filling requirements of the ions. The stabilities of the cations **6a**, **7b**, and **4a**, as expressed by their pK_{R+} values, have been determined in strongly basic non-aqueous solution by use of the C_- acidity function; the values obtained were 14.5, 19.4, and 23.7, respectively. This study further implied that the C_- scale in its present form is unsuitable for the precise determination of pK_{R+} values beyond 22.

Keywords: aromatic nucleophilic substitution · carbocations · nitrogen heterocycles · pK_{R+} values · solid-state structures

Introduction

Stabilized carbenium ions such as the triarylmethylium, xanthenium, and acridinium cations are organic compounds of great scientific and commercial importance. Many of them are used as textile and laser dyes, as well as in various fluorescent probes and cellular stains for biological and clinical purposes.[1–3] Consequently, their thermodynamic and photophysical properties have been extensively studied, and great effort has been directed towards clarifying the relationship between structure and stability[4, 5] as well as towards synthesizing new carbenium ions with very high stabilities.[6, 7]

In our previous work on highly stable carbenium ions, we explored aromatic nucleophilic substitution (S_NAr) on methoxy-substituted carbenium ions with secondary amines, and found this to be an efficient means of preparing a variety of new carbenium ions,[8] including the exceptionally stable tris(diethylamino)trioxatriangulenium ion, $(Et_2N)_3$-TOTA$^+$. The fact that triarylcarbenium ions which bear *para*-chloro or *para*-methoxy substituents undergo aromatic nucleophilic substitution (S_NAr) with alcohols or amines as the nucleophiles has been known for some time.[9–11] However, preparative use of the facile S_NAr reaction of triaryl carbenium ions with amines has hitherto been limited to the *para* position, and no substitution of *ortho* functionalities has been reported, despite the fact that such isomers were present in the studied carbenium ions.[8, 11, 12] The present work was initiated in order to ascertain whether the S_NAr reaction could be applied to the *ortho* positions and, thereby, provide a synthetic route to the first nitrogen-bridged triangulenium ions, for example, the triazatriangulenium system (R′$_3$-TATA$^+$).

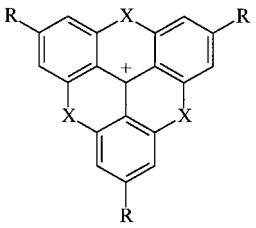

	X	R
$(Et_2N)_3$TOTA$^+$	O	Et_2N
R'$_3$-TATA$^+$	NR'	H
TOTA$^+$	O	H

Since Martin and Smith[13] described the synthesis of the trioxatriangulenium ion (TOTA$^+$) in 1964, this compound has been the subject of some attention due to its properties as a stable carbenium ion[14–18] and in the radical and dimeric states.[19–22] In recent years, the triangulene skeleton has been

[a] B. W. Laursen, Dr. F. C. Krebs
The Macromolecular Chemistry Group
Condensed Matter Physics and Chemistry Department
Risø National Laboratory, 4000 Roskilde (Denmark)
Fax: (+45) 4677 4791
E-mail: bo.laursen@risoe.dk

used in the construction of macrocyclophanes[23–25] and in stable triplet π biradicals.[26, 27] The TOTA$^+$ cation intercalates into double and triple helical DNA, where it acts as a photonuclease,[28] while the pyroelectric phosphangulene[29, 30] and other triangulene derivatives have been extensively studied in the solid state.[31, 32]

Changing the bridge atom in heterocyclic carbenium ions from oxygen to nitrogen significantly increases the cation stability. Hence, on going from the 9-phenyl-xanthenium ion ($pK_{R+} = 1.0$)[5] to the 10-methyl-9-phenyl-acridinium ion ($pK_{R+} = 11.0$)[33] (Figure 1), the stability increases by ten pK_{R+} units. With this in mind, the replacement of one, two, or even three oxygen bridges in the already highly stable TOTA$^+$ cation ($pK_{R+} = 9.1$)[13] with nitrogen could be expected to result in carbenium ions with very high pK_{R+} values. Indeed, we have shown this to be true, as we recently reported in a short communication.[34] In this paper, we report the results of a thorough investigation of the synthetic pathways leading to the various oxygen- and/or nitrogen-bridged triangulenium salts by the S_NAr approach. For these new carbenium salts, structural and spectroscopic properties as well as pK_{R+} values and the methods for their determination are also discussed.

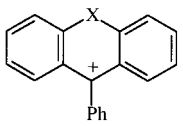

Figure 1. X = O: 9-phenylxanthylium ion; X = CH_3-N: 10-methyl-9-phenylacridinium ion.

Results and Discussion

Synthesis: The starting material for our exploration of the synthetic pathways leading to the nitrogen-containing triangulenes was the tris(2,6-dimethoxyphenyl)carbenium tetrafluoroborate **1-BF$_4$**, which was obtained in excellent yields from the corresponding carbinol. We found that the *ortho*-methoxy groups in this carbenium ion (**1**) do indeed undergo substitution upon treatment with primary amines, as outlined in Scheme 1 (reactions Ia, Ib, and Ic).[34] By controlling the reaction conditions, it is possible to obtain products in which two, four, or six of the *ortho*-methoxy groups of **1** are substituted, resulting in one, two, or three nitrogen bridges, respectively (compounds **2**, **3**, and **4**).

The S_NAr reactions of **1-BF$_4$** with primary amines were carried out in polar solvents such as 1-methyl-2-pyrrolidinone (NMP) or acetonitrile. At room temperature, the reactions between **1** and primary alkyl- and benzylamines proceeded rapidly (Scheme 1, reaction Ia) and the acridinium salts **2a-PF$_6$**, **2b-PF$_6$**, and **2d-PF$_6$** were isolated in good yields (73–78%). The substitution reaction leading to formation of the nitrogen bridges is believed to be a double S_NAr reaction, in which carbenium ion **1** first reacts with a primary amine with substitution of one of the *ortho*-methoxy groups. The next step is an intramolecular S_NAr reaction, in which an *ortho*-methoxy group on one of the neighbouring rings is substituted, thereby leading to ring-closure and the formation of a nitrogen bridge (Scheme 2).

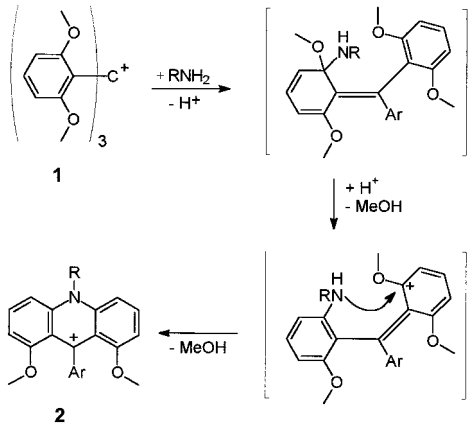

Scheme 2. Formation of the acridinium ions **2** from **1** and a primary amine occurs through a double S_NAr reaction with elimination of two equivalents of methanol; Ar = 2,6-dimethoxyphenyl.

Formation of the second nitrogen bridge demands higher temperatures, hence the doubly bridged compound **3b-BF$_4$** was obtained in 77% yield by heating **1-BF$_4$** with an excess of *n*-propylamine in NMP at 100 °C for 45 minutes (Scheme 1, reactions Ia and Ib).

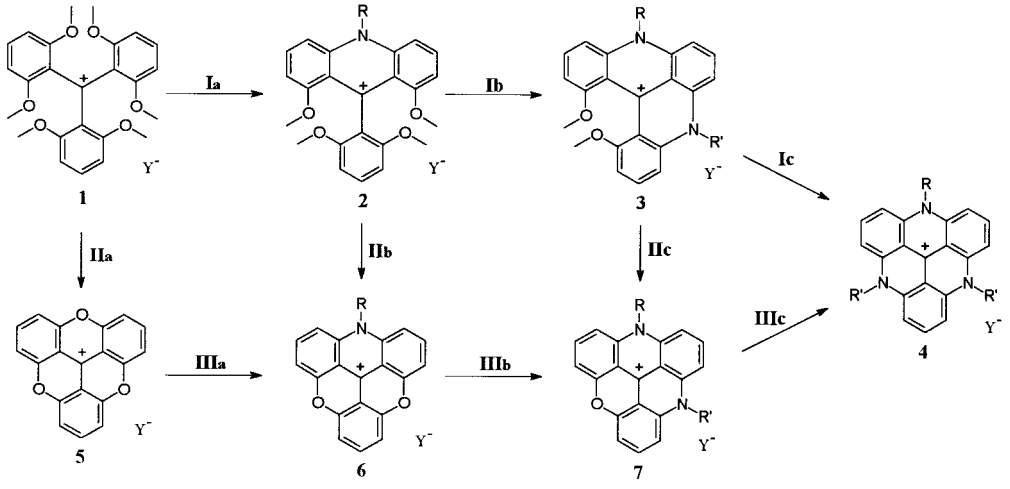

Scheme 1. Three types of S_NAr reactions (types I, II, and III) are found to take place in the transformations of **1** into **4**; **a**: R = R′ = Me, **b**: R = R′ = *n*-Pr, **c**: R = R′ = *n*-oct, **d**: R = Bz, **e**: R = Ph, **f**: R = *n*-Pr, R′ = *n*-oct; **Y**$^-$ = BF_4^- or PF_6^-.

0947-6539/01/0708-1774 $ 17.50+.50/0 *Chem. Eur. J.* **2001**, *7*, No. 8

Salts of the triply nitrogen-bridged triazatriangulenium ions (R_3-TATA$^+$) **4** were obtained after heating to even higher temperatures for longer times; the tri-*n*-octyl derivative **4c-BF$_4$** was obtained by refluxing **1-BF$_4$** in a mixture of NMP and *n*-octylamine for 24 hours. The required reaction temperatures for the formation of the R_3-TATA$^+$ ions (**4**) could not be achieved with low boiling amines such as methyl- and *n*-propylamine; however, when the reaction mixtures were buffered with benzoic acid, allowing the reflux temperature to be raised sufficiently, the formation of **4a** and **4b** could be achieved within 10–24 hours.

The decrease in reactivity associated with each subsequent introduction of a nitrogen bridge, which makes it possible to obtain the partially substituted compounds **2** and **3**, may be explained by considering the redistribution of the positive charge following each bridge formation. Thus, upon bridge formation, the methoxy groups are replaced by more strongly electron-donating alkyl nitrogen moieties and the size of the coplanar ring system increases. As a result, the positive charge becomes more delocalized and consequently the electrophilicity of the remaining methoxy-substituted *ortho* positions is reduced. Furthermore, if the ring-forming S_NAr reactions are irreversible, their stepwise nature may also allow the synthesis of asymmetrical compounds through multistep reactions with different amines. This possibility was tested by treating the 10-*n*-propyl-acridinium salt **2b-PF$_6$** with a large excess of *n*-octylamine (reflux for 24 hours); this yielded the asymmetrically substituted TATA$^+$ salt **4f**. No evidence of the presence of the tri-*n*-octyl analogue **4c** was observed; the mass spectrum of the crude reaction mixture showed no peak attributable to **4c** (*m*/*z* 618), but only those due to **4f** (*m*/*z* 548) and products with lower *m*/*z*. This proves that the introduction of alkyl nitrogen bridges is practically irreversible under the applied conditions, and that the S_NAr approach is indeed suitable for the synthesis of more complex asymmetrical structures.

The formation of tri-*n*-octyl-TATA$^+$ **4c** was monitored by mass spectrometry. As expected, we observed a consecutive transformation of **1** to **3c** via **2c** (Scheme 1, reactions Ia and Ib), although at this stage the mass spectra showed that **3c** was converted to **7c** rather than directly to **4c** (see Figure 2). In conclusion, the formation of **4** from **3** proceeds mainly via **7**, that is, it involves an initial intramolecular ring closure (Scheme 1, reaction IIc) followed by substitution of the bridging oxygen atom by a primary amine (Scheme 1, reaction IIIc). The first step in this sequence corresponds to the thermal-[35] or nucleophilic-catalyzed[8, 13] intramolecular formation of oxygen bridges in the synthesis of the TOTA$^+$ cation **5** (Scheme 1, reaction IIa). The substitution of oxygen bridges (Scheme 1, reaction IIIc) is analogous to the known transformation of pyrylium compounds into pyridinium salts by reaction with amines.[36] This last type of substitution must involve a nucleophilic attack at the 3-position of the TOTA$^+$ system. This is in agreement with theoretical calculations, which predicted that a substantial fraction of the total positive charge of the cation should reside in this position.[37]

The reaction sequence discussed above highlights the competition between inter- and intramolecular substitution

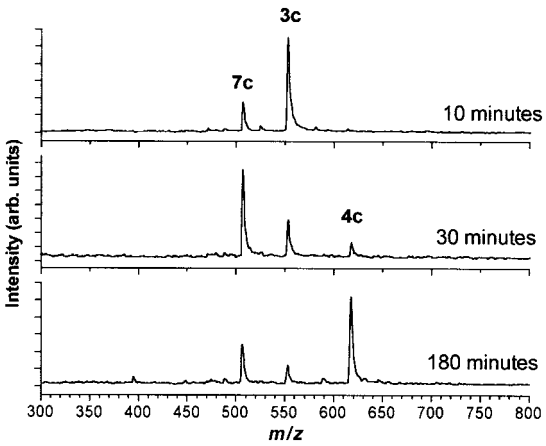

Figure 2. MALDI-TOF mass spectra of the crude reaction mixture from the synthesis of **4c-PF$_6$**. The spectra were recorded after refluxing **1-BF$_4$** in NMP/*n*-octylamine for 10, 30, and 180 min. On the basis of the mass spectra, it is not possible completely to rule out the direct transformation of **3** into **4**; we can merely state that at a certain time during the reaction (30 min.) the ratio between **7c** and **4c** was approximately 10:1 based on the peak intensities. Similar observations were made in relation to the synthesis of **4a** and **4b** from **1-BF$_4$**.

in the *ortho*-methoxy-substituted triaryl carbenium ions (reaction paths I and II, respectively). The key factors that determine the reaction path are the reaction temperature, the nucleophilicity, and the concentration of the amine. This is illustrated by the reaction of **1** with aniline, which is a weaker nucleophile. The formation of only one nitrogen bridge was observed before intramolecular ring-closure became the dominant reaction. Thus, the azadioxatriangulenium salt **6e-BF$_4$** was obtained in one synthetic step, simply by refluxing **1-BF$_4$** in pure aniline.

Substitution of the oxygen bridges in the triangulenium ions (reaction type III) was confirmed by the observation that tri-*n*-octyl-TATA$^+$ **4c** can also be synthesized starting from the TOTA$^+$ cation **5**, simply by heating the latter with *n*-octylamine (Scheme 1, reactions IIIa–IIIc). However, for this reaction sequence, mass spectrometry showed that only a small amount of the mono-substituted product **6c** was present during the transformation of **5** into the disubstituted product **7c**. This behavior can be explained in terms of competing reversible nucleophilic attack at the central carbon in the triangulenium system (12c position) yielding the leuco compound. Thus, when an excess of an amine was added to a solution of **5**, the nonionic and nonreactive leuco adduct was formed immediately; dissociation only occurred upon heating, regenerating a small "steady-state" concentration of the reactive cation **5**, which underwent substitution to give **6**. Due to the lower electrophilicity of the central carbon atom of cation **6** (see Table 1, later), the formation of the leuco adduct of this cation is less significant, and **6** was quickly transformed into **7**. This complication does not arise in reactions starting from carbenium salt **1** owing to the steric bulk of the six *ortho*-methoxy groups that surround and shield the central carbon atom in the carbenium ion of **1**.

The partially nitrogen-bridged compounds **2a** and **3b** were converted into the fully ring-closed azadioxa- and diazaoxatriangulenium salts **6a** and **7b** in good yields (80 and 85%,

respectively) upon heating with pyridine hydrochloride (reactions IIb and IIc). While the use of molten pyridine hydrochloride resulted in pronounced *N*-dealkylation of the diethylamino-substituted trioxatriangulenium cation $(Et_2N)_3$-TOTA$^+$,[8] no evidence for such a reaction was observed in the preparation of compounds **6a** and **7b**, with R being an alkyl group. However, cleavage of the benzylic group in compound **2d** was achieved, together with ring-closure, by treatment with molten pyridine hydrochloride. Upon basic work-up, the novel nonionic heteroaromatic azadioxatriangulene **8** was isolated in 77% yield (Scheme 3). Compound **8** was found to be only slightly soluble in dichloromethane and chloroform and insoluble in most other solvents. However, recrystallization from hot 1,2-dichlorobenzene yielded beautiful orange needles of sufficient quality for X-ray analysis.

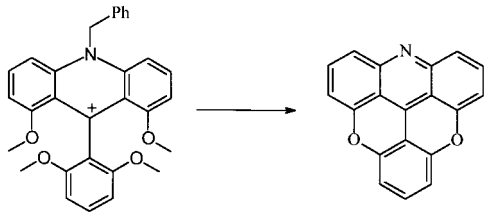

2d **8**

Scheme 3. Treatment of the 10-benzylacridinium salt **2d-PF$_6$** with molten pyridine hydrochloride followed by basicification with H_2O/KOH yields the neutral acridine analogue **8**.

Molecular and crystal structures: Crystals of sufficient quality for X-ray crystal structure determinations were obtained for the compounds **2b-PF$_6$**, **2d-PF$_6$**, **4b-BF$_4$**, **4c-BF$_4$**, **6e-BF$_4$**, and **8**. These structures, together with previously reported X-ray studies on a large number of TOTA$^+$ salts[32] and their amino-substituted congeners,[38] for example, $(Et_2N)_3$-TOTA$^+$, provide an interesting basis for a discussion on the effect that charge delocalization has on the packing modes of these carbenium salts. These structures should allow us to ascertain whether the differences in the thermodynamic stabilities (pK_{R+} values) and spectroscopic properties seen for the various aza- and/or oxatriangulenium ions are related to changes in the geometry of the triangulenium skeleton, or whether these effects are mainly of an electronic nature.

The most characteristic feature of the two methoxy-substituted acridinium salts **2b-PF$_6$** and **2d-PF$_6$** is the torsion angle between the 2,6-dimethoxyphenyl substituent and the acridine system, which is close to 90° in both cases (92.976° for **2b** and 94.015° and 94.704°, respectively, for the two molecules in the asymmetric unit of **2d**). This perpendicular arrangement of the two ring systems can be attributed to the steric bulk of methoxy substituents and, as a result, the 2,6-dimethoxyphenyl substituent is essentially electronically isolated from the acridinium system. This observation is supportive of the fact that the acridinium derivatives **2** are formed very quickly under the reaction conditions, but that the subsequent formation of the second nitrogen bridge requires higher temperatures in order to overcome the rotational barrier and bring the dimethoxyphenyl group into a favorable position for ring formation. A stereoview of **2d** is included in Figure 3 to emphasize this point.

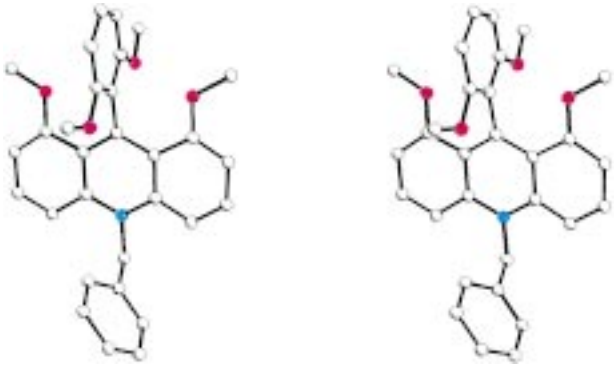

Figure 3. A stereoview of compound **2d** showing the orthogonality of the 2,6-dimethoxy substituent with respect to the acridinium system.

When we recently reported the first nitrogen-bridged triangulenium salt **4a-PF$_6$**, no structural detail was provided due to a disorder in the crystals (static or dynamic).[34] The small size of the methyl groups gives the molecule a near perfect disc shape, which hampers the formation of well-ordered crystals. However, a structure likely to contain pure cationic stacks with a periodicity of 3.5 Å was established from analysis of Weissenberg films. When the alkyl substituents on the R_3-TATA$^+$ are made longer, however, it becomes possible to grow crystals for which the structure can be solved. In the case of the tri-*n*-propyl compound **4b-BF$_4$**, the cations form staggered dimers. The staggering forces the alkyl groups away from the plane of the ring system such that the dimers become isolated, but the extensive $\pi-\pi$ overlap results in a close interplanar distance in the system. While the molecular symmetry in **4b-BF$_4$** is reflected in the space-group symmetry, the extension of the alkyl groups to *n*-octyl as in compound **4c-BF$_4$** breaks this symmetry and a triclinic space group is obtained. The molecules still arrange in staggered dimers with extensive $\pi-\pi$ overlap and a close interplanar distance. The mean interplanar distances in **4b-BF$_4$** and **4c-BF$_4$** are 3.29 and 3.38 Å, respectively. Stereoviews of the dimers are shown in Figure 4. On examining the changes in molecular conformation that take place on going from the *n*-propyl to the *n*-octyl derivative, it becomes clear that the alkyl groups are responsible for the symmetry breaking. In **4b-BF$_4$**, the *n*-propyl chains extend in a direction away from the aromatic center, consistent with the threefold symmetry of the molecule, whereas in **4c-BF$_4$** the *n*-octyl groups extend away from the plane of the aromatic system but in a common direction, which is inconsistent with the threefold molecular symmetry. This is emphasized in Figure 5, in which the two molecules have been overlaid. One possible explanation for the symmetry breaking is the simultaneous accommodation of the anions and the alkyl chain. The cationic aromatic core of the dimer would ideally surround itself with anions to minimize the electrostatic potential, as is indeed observed in the packing of **4b-BF$_4$**, in which the dimers pack in trigonal

  0947-6539/01/0708-1776 $ 17.50+.50/0 *Chem. Eur. J.* **2001**, *7*, No. 8

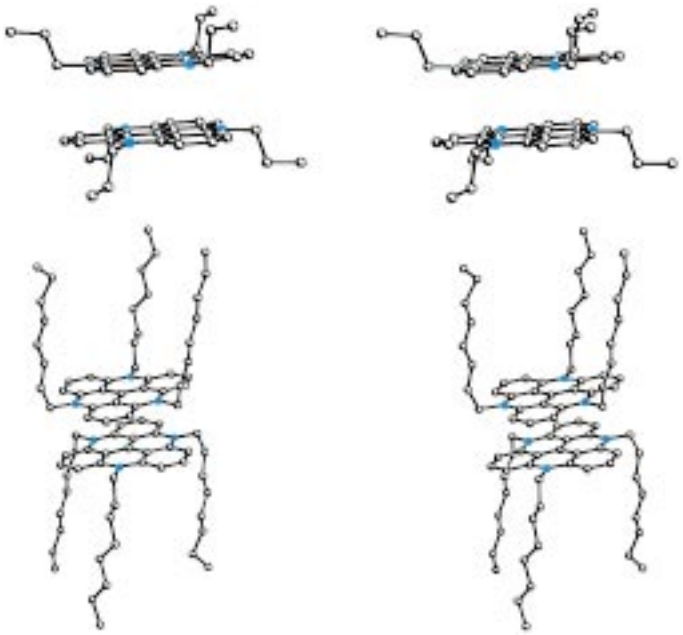

Figure 4. Stereoview showing the staggered dimers of compounds **4b-BF$_4$** (above) and **4c-BF$_4$** (below). It can clearly be seen that the staggered nature of the dimer forces the alkyl substituent away from the molecular plane.

planes as shown in Figure 6. The dimer assemblies are surrounded by tetrafluoroborate ions in the plane and above and below the dimer. As the alkyl chain is made longer, it becomes impossible to accommodate both the ions and the hydrophobic chains and a kind of phase separation is observed. Thus, a layered structure is formed, made up of alternate layers of hydrophobic alkyl chains that include disordered solvent molecules and ionic dimer layers that contain the tetrafluoroborate ions, as shown in Figure 7. This structure bears a striking resemblance to the structures of many detergents and lamellar liquid crystals. The slightly larger interplanar distance observed in the dimer of **4c-BF$_4$** as compared to **4b-BF$_4$** may also be explained in terms of the separation into a lamellar or layered structure; the effect of placing two cations in a dimeric structure is not so effectively screened in **4c-BF$_4$** as it is in **4b-BF$_4$**, hence a slight increase in interplanar distance results.

We also report the azadioxa derivatives **6** (ADOTA$^+$) and **8** (ADOTA), in which the interesting possibility exists of having the planar system in both cationic and neutral forms. Both the ADOTA and ADOTA$^+$ systems are planar molecules that exhibit close interplanar distances in the solid state. In the case of **6e-BF$_4$**, a dimer is again observed, as shown in Figure 8. The interplanar distance observed in the dimer of **6e-BF$_4$** is 3.316 Å and is thus comparable to that observed for **4b-BF$_4$**, consistent with an equal distribution of the surrounding anions. In the neutral compound **8**, infinite directional chains are observed with a significant interaction between the molecular dipoles through an Ar–CH$\cdots$N interaction (C–N distance 3.439 Å) as compared to the corresponding Ar–CH$\cdots$O interaction (C–O distance 3.699 Å). Figure 9 shows the chains of **8**, in which the interplanar distance between the aromatic systems is 3.330 Å. This is somewhat longer than the corresponding distances observed in **4b-BF$_4$** and **6e-BF$_4$**, but shorter than that in **4c-BF$_4$**. This suggests that the attractive $\pi-\pi$ interaction in **4b-BF$_4$** and **6e-BF$_4$** is larger than that in compound **4c-BF$_4$**. No evidence was found for rotational disorder of the molecules in the crystal; this observation can be ascribed to the dipolar and specific hydrogen interactions of the molecule. While both TOTA$^+$ and Me$_3$-TATA$^+$ have been considered to rotate in the crystal at elevated temperatures,[32,34] and possibly at room temperature in the case of the Me$_3$-TATA$^+$ derivative,[34] it was of interest to ascertain whether there were any significant differences in the molecular structures of the aromatic cores in TOTA$^+$, TATA$^+$, ADOTA, and ADOTA$^+$. A thorough

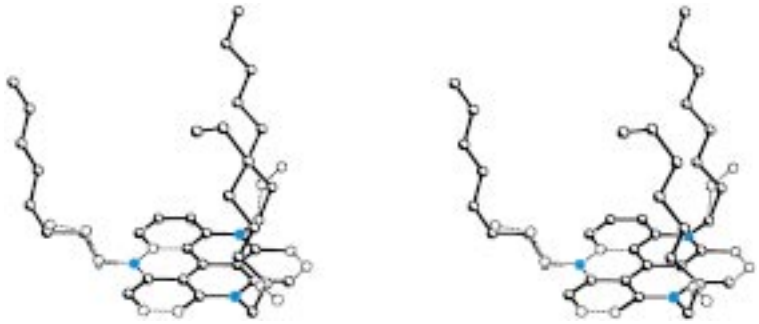

Figure 5. Cations **4b** and **4c** overlaid (stereoview) to show the similarities/differences between the two molecules as observed in the solid state. Notice how one of the *n*-octyl groups corresponds to the *n*-propyl group, whereas the other two take a different direction and break the symmetry.

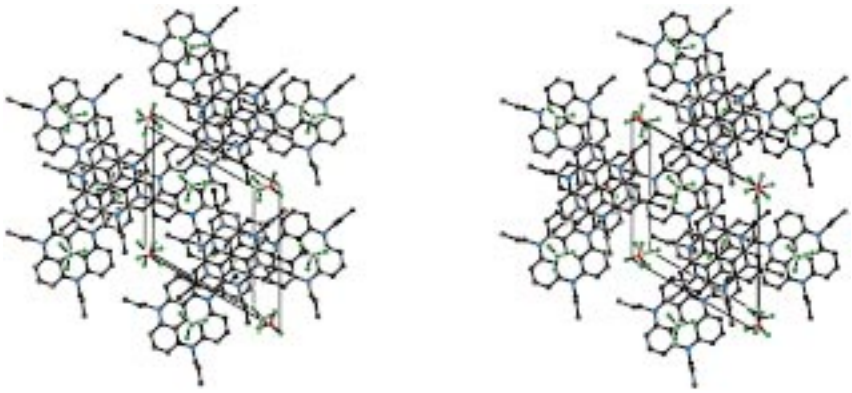

Figure 6. A stereoview of the packing in compound **4b-BF$_4$**. Notice how the anions are well distributed in the crystal. In fact, pairs of anions are situated in pockets that also contain one disordered acetonitrile solvent molecule.

Figure 7. A stereoview of the packing observed for compound **4c-BF$_4$**. Notice how the ionic parts and the alkyl chains separate into layers (the layers containing the alkyl groups include disordered acetonitrile solvent molecules).

Figure 8. A stereoview of the dimers observed for the cationic compound **6e** (anion not shown). Notice how there is still some aromatic overlap.

Figure 9. A stereoview of the infinite linear chains observed for compound **8**. There is some interaction between the nitrogen atoms and the aromatic part of neighboring molecules.

analysis, in which the aromatic cores were fitted to one another, revealed no significant differences. The triangulene system retains its formal geometrical planarity and threefold symmetry whether cationic or neutral, oxygen- or nitrogen-containing, and even if the symmetry is broken by having different atoms in the 4-, 8-, and 12-positions as in **6e** and **8**.

Electronic absorption spectra: While the absorption spectra of the partially ring-closed cations **2a** and, in particular, **3b** are strongly influenced by the molecular conformation, in terms of nonplanar chromophores[34] the fully ring-closed triangulenium ions **5**, **6**, **7**, and **4** are all coplanar. Thus, variations in the electronic absorption spectra can be ascribed solely to the changes in the electronic structure resulting from the substitution of the bridging heteroatoms. Absorption spectra of the four possible combinations of oxygen- and/or alkyl nitrogen-bridged triangulenium ions are shown in Figure 10.

All the triangulenium ions are characterized by moderately strong absorptions in the visible region ($8000 < \varepsilon < 20000\,M^{-1}cm^{-1}$), which are clearly separated from the somewhat stronger UV transitions that start to emerge below 370 nm. Comparison between the threefold-symmetrical triangulenium ions TOTA$^+$ and Me$_3$-TATA$^+$ shows that a change in the bridging heteroatom from oxygen to nitrogen is accompanied by a red shift of the order of 45 nm and a twofold intensity enhancement. While both TOTA$^+$ and Me$_3$-TATA$^+$ display one major band, with little or no structure, the less symmetrical cations **6a** and **7b** show broad structured bands in the visible region consisting of multiple peaks. In line with observations made for substituted triaryl carbenium dyes,[39] the broadness and structure of the visible absorption bands is clearly related to the symmetry of the ions. More surprising is the observed red shift on going from TOTA$^+$ to R$_3$-TATA$^+$; this is at variance with the trend seen in the case of the xanthenium and acridinium systems (Figure 1), in which changing the heteroatom from oxygen to nitrogen causes a blue shift of 30 nm.[40, 41]

The nonionic azadioxatriangulene **8**, which, from a structural point of view, may be considered as an extended acridine, displays a characteristic band in the visible region with a pronounced fine structure (Figure 11). The absorption spectrum of **8** resembles that of simple acridines with respect to bandshape and intensities, but the extension of the chromophoric system causes a red shift in the low-energy absorption band of almost 100 nm. While **8** was found to be insoluble in acetonitrile, the addition of hydrochloric acid resulted in immediate dissolution yielding a bright orange solution of the protonated form, which displayed an absorption spectrum closely resembling that of **6a** (see Figures 10 and 11).

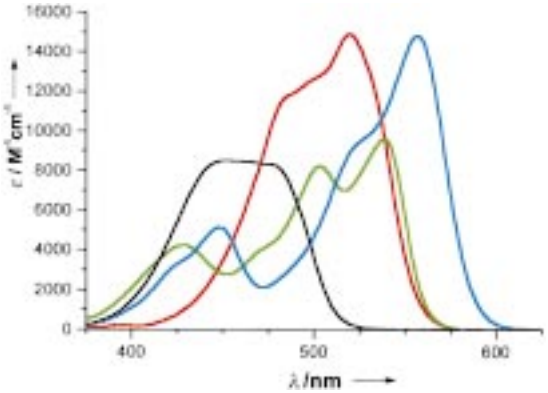

Figure 10. Absorption spectra of triangulenium salts measured in acetonitrile: **4a-PF$_6$** (red), **5-BF$_4$** (black), **6a-PF$_6$** (green), and **7b-PF$_6$** (blue).

pK_{R+} values: The affinity of the carbenium ion towards hydroxide ions, as expressed by the pK_{R+} value, is the most common measure of carbenium ion stability. When pK_{R+} values lie outside of the normal pH range, Hammett acidity functions are normally applied, that is, the H_R function for less stable carbenium ions.[4, 42] The evaluation of such acidity functions requires a series of overlapping indicators covering the range from aqueous solution through to the solvent system

0947-6539/01/0708-1778 $ 17.50+.50/0 *Chem. Eur. J.* **2001**, *7*, No. 8

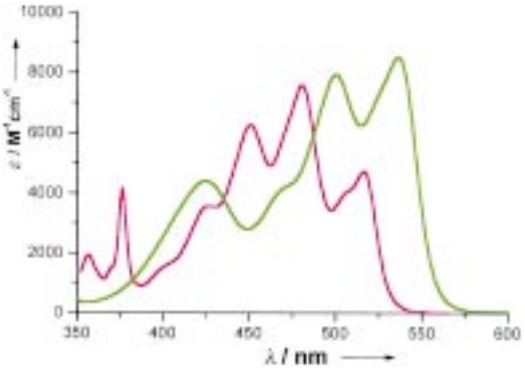

Figure 11. Absorption spectrum of azadioxatriangulene (**8**): neutral form measured in dichloromethane (magenta), cationic/protonated form in acetonitrile/aq. HCl (green).

employed, making it possible to observe responses of the activities to a change in solvent composition. By taking these changes in activity into account, the acidity function becomes an extension of the pH range. If the acidity function is valid, then for a particular compound the logarithm of the ratio between the acid and its base {in this case: log([ROH]/[R^+])} should change linearly with the acidity function, with a slope of unity.

When we needed an acidity function to determine the stability of the $(Et_2N)_3$-TOTA$^+$ ion,[8] a series of highly stable carbenium ions with pK_{R+} values above 14 was not available. Thus, the $C\_$ acidity function was constructed by modifying an existing acidity function $H\_$ based on a solvent system of DMSO/water/tetramethylammonium hydroxide.[43] The modification of $H\_$ was based on the observed proportionality between the slopes of the two functions in the ranges covered by the two carbenium ions at our disposal.[8]

The equilibria between the triangulenium ions **4a**, **6a**, and **7b** and their carbinols were studied by UV/Vis spectrophotometry in the DMSO/water/Me_4NOH solvent system. Like Ito and co-workers, who also used this solvent system for pK_{R+} measurements,[7] we experienced problems with the reversibility of the cation/carbinol reaction. Hence, on monitoring the absorption of the cations as a function of time following addition to the basic solutions, a continuous depletion of the signal was observed, accompanied by reduced recovery upon acidification. The rate of this reaction increases with the basicity of the solutions. The degradation of the carbinols, which is probably a result of reactions with the solvent at high basicity, indicates the limitations of this method. However, these problems were significantly reduced by careful deoxygenation of all solutions and by using a procedure which reduced the time frame of the experiments (see Experimental Section). By employing this procedure, more than 96% of the absorbance of the carbenium ions was recovered upon acidification following each equilibrium measurement. For the azadioxa- and diazaoxatriangulenium ions **6a** and **7b**, we determined pK_{R+} values of 14.5 and 19.4, respectively. For these two cations, the equilibrium measurements showed very good correlations with the $C\_$ function, i. e. good linearity and slopes very close to unity (Figure 12 and Table 1). In the case of the Me_3-TATA$^+$ ion **4a**, the slope was only 0.85, which may indicate a change in the slope of the $C\_$ function relative to the underlying $H\_$ function. However, a pK_{R+} value of approximately 23.7 can be estimated for **4a**.[34] In conclusion, the behavior of compounds **6a** and **7b** supports the validity of the $C\_$ function in the region below 70 mol% DMSO ($C\_ = 21.5$), while the reliability of the $C\_$ function and the solvent system at higher basicity is doubtful.

Table 1. Stability of triangulenium ions in terms of their pK_{R+} values.

Compound	pK_{R+}	Notes
4a	23.7	$C\_$, slope 0.85
5	9.1	aqueous solution[a]
6a	14.5	$C\_$, slope 1.02
7b	19.4	$C\_$, slope 1.01

[a] Ref. [13].

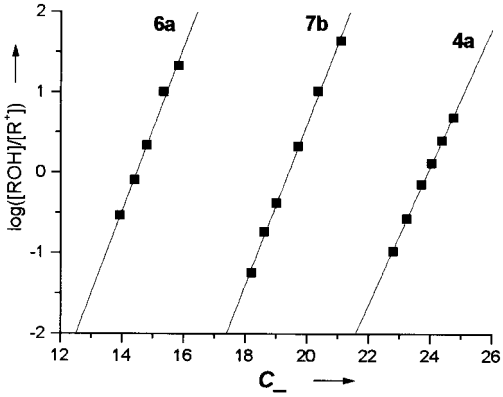

Figure 12. Linear fits to log([ROH]/[R^+]) versus $C\_$ for compounds **6a**, **7b**, and **4a**.

Regardless of the uncertainty in the exact pK_{R+} value of **4a**, the stabilities of the three azatriangulenium ions confirm the considerable stabilizing power of nitrogen bridges in these carbenium salts. Thus, the introduction of one nitrogen bridge into TOTA$^+$ (**5**) results in an increase in stability of 5.4 pK units. The stabilizing effect seems to be additive with only a moderate saturation effect,[44] hence $\Delta pK_{R+} = 5.4$, 4.9, and 4.3 for the three oxygen to nitrogen substitutions, respectively. The extreme stability of the Me_3-TATA$^+$ ion **4a** places it among the most stable known carbenium ions, comparable with the bis- and tris(dimethylamino)-substituted triazulenyl carbenium ions recently synthesized by Ito and co-workers.[7] For these cations, Ito and co-workers reported pK_{R+} values of 21.4 and 24.3, respectively, on the $H\_$ scale, which roughly correspond to values of 24 and 27, respectively, on the $C\_$ scale, ignoring the uncertainty in the scale in this region. A valid comparison of these values with the pK_{R+} values of other superstable carbenium ions also becomes difficult for two other reasons: 1) Ito and co-workers do not report how the equilibria of the two cations with their carbinols respond to changes in the solvent composition, that is, the slope of log ([ROH]/[R^+]) *vs.* the appropriate acidity function ($H\_$ or $C\_$), and 2) the measurements were apparently performed under conditions where the reaction was not reversible.

Conclusion

In this paper, we have reported the simple and facile synthesis of three new types of nitrogen-bridged carbenium salts of the triangulenium family. Various derivatives of the mono-, di-, and triazatriangulenium salts **6**, **7**, and **4** have been obtained by simple one- or two-step procedures from the common precursor **1**. The aromatic nucleophilic substitution reactions that are the key steps in these syntheses offer, owing to their stepwise nature and irreversibility, a powerful means for the preparation of new nitrogen-bridged carbenium salts. Our investigation of the synthetic pathways involved in the formation of the carbenium salts **2**–**7** from **1** has revealed that three types of S_NAr reactions can take place. The first type is a double S_NAr reaction, in which two *ortho*-methoxy groups on different aryl substituents are replaced by one primary alkyl-, aryl-, or benzylamine (type I). Secondly, an intramolecular S_NAr reaction in which methoxy groups act as both the nucleophile and the leaving group is possible, which leads to the formation of oxygen bridges (type II). The third possibility is nucleophilic attack and replacement of oxygen bridges by primary amines (type III).

The solid-state structures of four new triangulenes have been solved. The results, in conjunction with those of previous crystallographic studies, show that the conformation of the triangulenium skeleton is insensitive to whether the heteroatoms are oxygen and/or nitrogen. Hence, physical and chemical differences between the various triangulenium derivatives can be assigned to variations in the electronic structure. The crystal structures of the triazatriangulenium salts (**4**) show how the size of the alkyl substituents affects the packing mode, from the suggested segregated stacking in the methyl derivative **4a-PF$_6$**, to a dimeric structure for **4b-BF$_4$**, and finally to a lamellar-type structure for the tri-*n*-octyl derivative **4c-PF$_6$**. The observed packing modes indicate that the pronounced charge delocalization in the $TATA^+$ ion permits pure cationic stacking, but that, on the other hand, the steric requirements of the flanking alkyl groups generally prevent this.

The thermodynamic stabilities of the azatriangulenium ions were evaluated in terms of their pK_{R+} values. The data confirmed that the replacement of oxygen by nitrogen as the bridging heteroatoms in these carbenium salts efficiently increases the stability. Thus, substitution of all three oxygen bridges in the $TOTA^+$ cation **5** by nitogen results in the R_3-$TATA^+$ cations **4**, which in turn is accompanied by an increase in the stability constant by 14 orders of magnitude. The pK_{R+} values were evaluated by using an improved version of the recently suggested C_- acidity function,[8] and the measurements supported the essential validity of this method for determining pK_{R+} values below 22. However, the results also showed that the C_- function is inadequate for exact measurements of higher pK_{R+} values. Hence, the determination of exact pK_{R+} values for superstable carbenium ions will require the evaluation of a new method that is not based on the solvent systems currently in use.

Experimental Section

Synthetic methods and materials: All reagents used were standard grade unless specified otherwise. NMR spectra were recorded on a Bruker 250 MHz spectrometer. UV/Vis spectra were obtained on a Perkin–Elmer Lambda 16 spectrophotometer. Elemental analyses were performed at the University of Copenhagen, Department of Chemistry, Elemental Analysis Laboratory, Universitetsparken 5, 2100 Copenhagen (Denmark). The syntheses of compounds **2a-PF$_6$**, **3b-BF$_4$**, and **4a-PF$_6$** are described in ref. [34] while that of **5-BF$_4$** can be found in ref. [32].

Tris(2,6-dimethoxyphenyl)carbenium tetrafluoroborate (1-BF$_4$): Aqueous HBF_4 solution (50%, 2.5 mL, 40 mmol) was added to a solution of tris(2,6-dimethoxyphenyl)carbinol[13] (5.8 g, 13.2 mmol) in absolute ethanol (100 mL). Diethyl ether (100 mL) was then added, followed by petroleum ether (100 mL, b.p. 40–60 °C). The dark-blue precipitate formed was collected by filtration and thoroughly washed with diethyl ether, yielding 6.5 g (97%) of greenish-black crystals. ^{1}H NMR ($CDCl_3$): $\delta = 7.62$ (t, ^3J(H,H) = 8.5 Hz, 3H), 6.56 (d, ^3J(H,H) = 8.5, 6H), 3.62 (s, 18H); ^{13}C NMR ($CDCl_3$): $\delta = 181.04$, 163.09, 142.87, 125.76, 105.37, 57.28; MS (MALDI-TOF): m/z: 423 $[M]^+$; UV/Vis (CH_2Cl_2): λ_{max} (lg ε) = 604 (4.08) (sh), 526 (4.26), 313 (3.45) (sh), 273 nm (4.06); elemental analysis calcd (%) for $C_{25}H_{27}O_6BF_4$: C 58.84, H 5.29; found C 58.79, H 5.21.

9-(2,6-Dimethoxyphenyl)-1,8-dimethoxy-10-*n*-propylacridinium hexafluorophosphate (2b-PF$_6$): Compound **1-BF$_4$** (1.0 g, 2 mmol) was dissolved in 1-methyl-2-pyrrolidinone (NMP) (15 mL), and *n*-propylamine (0.25 g, 4.2 mmol) was added. The initially purple reaction mixture immediately turned orange. After 20 h at room temperature, it was poured into aqueous KPF_6 solution (100 mL, 0.2 M) and the precipitate formed was collected by filtration and thoroughly washed with water. Recrystallization from methanol gave 0.85 g (75%) of dark-red needles of compound **2b-PF$_6$**. ^{1}H NMR (CD_3CN): $\delta = 8.22$ (dd, ^3J(H,H) = 8.1, 9.1 Hz, 2H), 7.94 (d, ^3J(H,H) = 9.2 Hz, 2H), 7.47 (t, ^3J(H,H) = 8.4 Hz, 1H), 7.1 (d, ^3J(H,H) = 8.0 Hz, 2H), 6.81 (d, ^3J(H,H) = 8.4 Hz, 2H), 5.04 (t, ^3J(H,H) = 8.6 Hz, 2H), 3.58 (s, 6H), 3.57 (s, 6H), 2.22 (m, 2H), 1.30 (t, ^3J(H,H) = 7.4 Hz, 3H); ^{13}C NMR (CD_3CN): $\delta = 160.47$, 157.09, 155.67, 141.55, 139.76, 129.76, 119.77, 119.54, 109.22, 106.38, 103.61, 56.66, 55.53, 53.64, 20.99, 9.99; MS (MALDI-TOF): m/z: 418 $[M]^+$; Elemental analysis calcd (%) for $C_{26}H_{28}NO_4PF_6$: C 55.42, H 4.97, N 2.48; found C 55.41, H 4.91, N 2.55.

9-(2,6-Dimethoxyphenyl)-1,8-dimethoxy-10-benzylacridinium hexafluorophosphate (2d-PF$_6$): Compound **1-BF$_4$** (3.0 g, 5.9 mmol) was dissolved in NMP (20 mL), and benzylamine (1.4 g, 13 mmol) was added. The reaction mixture immediately turned dark orange. After 1 h at room temperature, it was poured into aqueous KPF_6 solution (150 mL, 0.2 M) acidified with HPF_6 (60%, 2 g, 8 mmol), and the precipitate was collected by filtration and thoroughly washed with water. Recrystallization from methanol gave 2.8 g (78%) of orange-red crystals of compound **2d-PF$_6$**. ^{1}H NMR (CD_3CN): $\delta = 8.10$ (t, ^3J(H,H) = 9.0 Hz, 2H), 7.70 (d, ^3J(H,H) = 9.1 Hz, 2H), 7.42 (m, 4H), 7.20 (m, 2H), 7.09 (d, ^3J(H,H) = 8.1 Hz, 2H), 6.80 (d, ^3J(H,H) = 8.4 Hz, 2H), 6.33 (s, 2H), 3.59 (s, 6H), 3.56 (s, 6H); ^{13}C NMR (CD_3CN): $\delta = 160.65$, 158.73, 155.69, 142.35, 140.35, 133.49, 129.51, 129.23, 128.33, 125.77, 119.93, 119.37, 109.33, 106.66, 103.65, 56.75, 56.16, 55.58; MS (MALDI-TOF): m/z: 466 $[M]^+$; UV/Vis (CH_2Cl_2): λ_{max} (lg ε) = 535 (3.78) (sh), 506 (3.84), 411 (3.92), 354 (3.71), 340 (3.48), 287 nm (4.87); elemental analysis calcd (%) for $C_{30}H_{28}NO_4PF_6$: C 58.92, H 4.58, N 2.29; found C 58.70, H 4.53, N 2.26.

4,8,12-Tri-*n*-propyl-4,8,12-triazatriangulenium tetrafluoroborate (4b-BF$_4$): Compound **1-BF$_4$** (1.0 g, 2.0 mmol) was dissolved in NMP (30 mL), benzoic acid (5.2 g, 42 mmol) and *n*-propylamine (3.2 g, 54 mmol) were added, and the mixture was heated to reflux under argon for 20 h. Further *n*-propylamine (2 × 0.5 mL, 12 mmol) was added twice during the course of the reaction. After cooling to room temperature, the reaction mixture was poured into water, and the precipitate formed was collected by filtration and thoroughly washed with water. After drying, the crude product was thoroughly washed with diethyl ether and then recrystallized from acetonitrile to yield 0.35 g (32%) of red crystals. ^{1}H NMR (CD_3CN): $\delta = 7.97$ (t, ^3J(H,H) = 8.6 Hz, 3H), 7.15 (d, ^3J(H,H) = 8.6 Hz, 6H), 4.10 (t, ^3J(H,H) = 8.3 Hz, 6H), 1.85 (m, 6H), 1.67 (t, ^3J(H,H) = 7.4 Hz, 9H); ^{13}C NMR (CD_3CN): $\delta = 140.55$, 140.33, 138.00, 110.50, 105.48, 49.44, 18.41, 10.44; MS (MALDI-TOF): m/z: 408 $[M]^+$; elemental analysis calcd (%) for $C_{22}H_{18}N_3BF_4$: C 67.88, H 6.06, N 8.48; found C 67.88, H 6.14, N 8.75.

0947-6539/01/0708-1780 $ 17.50+.50/0 *Chem. Eur. J.* **2001**, *7*, No. 8

4,8,12-Tri-*n*-octyl-4,8,12-triazatriangulenium tetrafluoroborate (4c-BF_4)

From ***1-BF₄***: Tris(2,6-dimethoxyphenyl)carbenium tetrafluoroborate (**1-BF_4**) (1.0 g, 2.0 mmol) was dissolved in NMP (5 mL), and *n*-octylamine (12 g, 93 mmol) was added. The reaction mixture was refluxed for 24 h. After cooling, diethyl ether was added, and the red-orange crystalline precipitate formed was collected by filtration. Two recrystallizations from methanol yielded 0.62 g (44%) of red crystals. ^{1}H NMR (CD_3CN): $\delta = 7.91$ (t, $^3J(H,H) = 8.6$ Hz, 3H), 7.04 (d, $^3J(H,H) = 8.6$ Hz, 6H), 4.00 (t, $^3J(H,H) = 7.9$ Hz, 6H), 1.76 (m, 6H), 1.45 (m, 30H), 0.95 (t, $^3J(H,H) = 6.4$ Hz, 9H); ^{13}C NMR (CD_3CN): $\delta = 139.83$, 139.48, 137.53, 109.80, 104.91, 47.60, 31.45, 28.95, 28.84, 26.11, 24.35, 22.30, 13.32; MS (MALDI-TOF): *m*/*z*: 618 [M^+]; UV/Vis (MeCN): λ_{max} (lg ε) = 523 (4.26), 502 (4.17) (sh), 489 (4.14) (sh), 352 (3.85), 340 (3.79), 290 (4.38) (sh), 273 nm (4.95); elemental analysis calcd (%) for $C_{43}H_{60}N_3BF_4$: C 73.17, H 8.50, N 5.95; found C 73.16, H 8.69, N 5.86.

From ***5-BF₄***: Trioxatriangulenium tetrafluoroborate (**5-BF_4**) (0.25 g, 0.67 mmol) was dissolved in NMP (15 mL), and *n*-octylamine (4.0 g, 31 mmol) was added. The reaction mixture was refluxed under nitrogen for 8 h. It was then poured into aqueous KPF_6 solution (100 mL, 0.2 M) and extracted with CH_2Cl_2. The organic phase was washed with pure water and concentrated in vacuo; subsequent addition of diethyl ether and petroleum ether induced precipitation of the crude product. Recrystallization from ethanol gave 0.20 g (40%) of red crystals. The MS, ^{1}H NMR, ^{13}C NMR, and UV/Vis spectra were identical to those of the BF_4 salt. Elemental analysis calcd (%) for $C_{43}H_{60}N_3PF_6$: C 67.56, H 7.85, N 5.49; found C 67.66, H 7.88, N 5.53.

4,8-Di-*n*-octyl-12-*n*-propyl-4,8,12-triazatriangulenium hexafluorophosphate (4f-PF_6): Compound **2b-PF_6** (0.35 g, 0.62 mmol) was dissolved in NMP (20 mL), and *n*-octylamine (4.0 g, 31 mmol) was added. The reaction mixture was heated under reflux under nitrogen for 24 h. It was then poured into aqueous KPF_6 solution (100 mL, 0.2 M), and the resulting mixture was extracted with CH_2Cl_2. The organic phase was washed with pure water and concentrated in vacuo; subsequent addition of methanol (50 mL) induced precipitation of the crude product. Recrystallization from chloroform gave 0.13 g (30%) of the red-orange compound **4f-PF_6**. ^{1}H NMR (CD_3CN): $\delta = 7.93$ (m, 3H), 7.07 (m, 6H), 4.02 (m, 6H), 1.78 (m, 6H), 1.47 (m, 20H), 1.16 (t, $^3J(H,H) = 7.3$ Hz, 3H), 0.95 (t, $^3J(H,H) = 6.4$ Hz, 6H); ^{13}C NMR (CD_3CN): $\delta = 140.04$, 139.98, 139.70, 137.60, 109.97, 105.08, 105.00, 49.03, 47.68, 31.53, 29.02, 28.93, 26.20, 24.44, 22.83, 17.99, 13.40, 10.03 (due to overlap of the signals, only 7 of the expected 11 peaks in the aromatic region could be discerned); MS (MALDI-TOF): *m*/*z*: 548 [M^+]; the UV/Vis spectrum was identical to that of compound **4c-PF_6**; elemental analysis calcd (%) for $C_{38}H_{50}N_3PF_6$: C 65.78, H 7.20, N 6.05; found C 65.50, H 7.31, N 6.05.

4-Methyl-4-aza-8,12-dioxatriangulenium hexafluorophosphate (6a-PF_6): A solution of compound **3a-PF_6** (0.50 g, 0.93 mmol) in pyridine (6 mL) was added to molten pyridine hydrochloride (12 g). The reaction mixture was heated to approximately 200 °C for 1 h while the excess pyridine was allowed to distill off. The cooled residue was then dissolved in water (50 mL), and the crude product was precipitated by the addition of aqueous KPF_6 solution (100 mL, 0.2 M). The precipitate was collected by filtration, washed with pure water, and dried. The crude product was dissolved in warm acetonitrile; this solution was filtered, and then an equal volume of ethanol was added to the filtrate; 0.33 g (80%) of red-orange crystals was obtained by slow partial evaporation of the solvent. ^{1}H NMR (CD_3CN): $\delta = 8.32$ (t, $^3J(H,H) = 8.6$ Hz, 2H), 8.07 (t, $^3J(H,H) = 8.5$ Hz, 1H), 7.79 (d, $^3J(H,H) = 8.9$ Hz, 2H), 7.48 (d, $^3J(H,H) = 8.2$ Hz, 2H), 7.40 (d, $^3J(H,H) = 8.5$ Hz, 2H), 4.17 (s, 3H); ^{13}C NMR (CD_3CN): $\delta = 152.54$, 151.88, 140.80, 140.74, 139.82, 111.49, 110.30, 109.25, 107.97, 104.89, 35.98 (due to overlap of the signals, only 10 of the expected 11 peaks in the aromatic region could be discerned); MS (MALDI-TOF): *m*/*z*: 298 [M^+]; UV/Vis (MeCN): λ_{max} (lg ε) = 539 (3.99), 503 (3.92), 473 (3.62) (sh), 429 (3.63), 329 (3.31), 315 (3.87) (sh), 299 (4.47), 259 (4.78); elemental analysis calcd (%) for $C_{20}H_{12}NO_2PF_6$: C 54.18, H 2.71, N 3.16; found C 54.31, H 2.45, N 3.16.

4-Phenyl-4-aza-8,12-dioxatriangulenium tetrafluoroborate (6e-BF_4): A mixture of compound **1-BF_4** (1.0 g, 2 mmol) and aniline (12 g) was heated to reflux for 4 h. The cooled reaction mixture was then poured into diethyl ether and the precipitate formed was collected by filtration, washed with diethyl ether, and dried. The crude product was dissolved in warm acetonitrile, the resulting solution was filtered, and then an equal volume of ethanol was added to the filtrate; 0.47 g (53%) of red-orange needles was obtained by slow partial evaporation of the solvent. ^{1}H NMR (CD_3CN): $\delta = 8.14$ (m, 3H), 7.88 (m, 3H), 7.56 (m, 6H), 6.90 (d, $^3J(H,H) = 8.8$ Hz, 2H); ^{13}C NMR (CD_3CN): $\delta = 152.75$, 152.58, 141.98, 141.62, 140.64, 140.17, 136.67, 131.83, 131.19, 127.83, 111.74, 111.13, 109.37, 108.36, 105.65; MS (MALDI-TOF): *m*/*z*: 360 [M^+]; UV/Vis (MeCN): λ_{max} (lg ε) = 539 (4.06), 504 (3.97), 473 (3.65) (sh), 433 (3.66), 316 (4.01) (sh), 299 (4.50), 259 nm (4.70); elemental analysis calcd (%) for $C_{25}H_{14}NO_2BF_4$: C 67.14, H 3.13, N 3.13; found C 67.03, H 2.90, N 3.24.

4,8-Di-*n*-propyl-4,8-diaza-12-oxatriangulenium hexafluorophosphate (7b-PF_6): A solution of compound **3b-BF_4** (0.65 g, 1.30 mmol) in pyridine (5 mL) was added to molten pyridine hydrochloride (20 g). The reaction mixture was heated to approximately 200 °C for 1 h, while the excess pyridine was allowed to distill off. The cooled reaction mixture was then dissolved in water (50 mL), and the crude product was precipitated by the addition of aqueous KPF_6 solution (100 mL, 0.2 M). The precipitate was collected by filtration, washed with pure water, and dried. The crude product was dissolved in warm acetonitrile, this solution was filtered, and then a twofold volume excess of absolute ethanol was added to the filtrate. Crystallization was induced by concentration of the solution; 0.57 g (85%) of dark-red crystals was obtained. ^{1}H NMR (CD_3CN): $\delta = 8.05$ (t, $^3J(H,H) = 8.6$ Hz, 1H), 7.81 (t, $^3J(H,H) = 8.5$ Hz, 2H), 7.23 (t, $^3J(H,H) = 8.9$ Hz, 4H), 6.91 (d, $^3J(H,H) = 8.2$ Hz, 2H), 4.10 (t, $^3J(H,H) = 8.2$ Hz, 4H), 1.75 (m, 4H), 1.07 (t, $^3J(H,H) = 7.4$ Hz, 6H); ^{13}C NMR (CD_3CN): $\delta =$ 152.13, 140.54, 139.54, 139.40, 139.19, 138.42, 111.17, 109.09, 108.27, 107.07, 105.77, 49.11, 18.70, 9.98; MS (MALDI-TOF): *m*/*z*: 367 [M^+]; UV/Vis (CH_2Cl_2): λ_{max} (lg ε) = 556 (4.17), 524 (3.97) (sh), 448 (3.71), 426 (3.53) (sh), 359 (3.48), 294 (4.32), 265 nm (4.87); elemental analysis calcd (%) for $C_{25}H_{23}N_2OPF_6$: C 58.59, H 4.49, N 5.46; found C 58.46, H 4.37, N 5.47.

4-Aza-8,12-dioxatriangulene (8): A solution of compound **2d-PF_6** (1.0 g, 1.6 mmol) in pyridine (5 mL) was added to molten pyridine hydrochloride (12 g). The reaction mixture was heated to approximately 200 °C for 4 h, while the excess pyridine was allowed to distill off. The cooled reaction mixture was then dissolved in water (50 mL) and basified with aqueous KOH solution. The precipitate formed was collected by filtration, washed with pure water, and dried. The crude product was dissolved in hot NMP and this solution was filtered; slow cooling of the filtrate yielded 0.35 g (77%) of orange hairlike crystals. Due to its low solubility, no ^{13}C NMR spectrum of this compound could be obtained. ^{1}H NMR ($CDCl_3$): $\delta = 7.70$ (m, 4H), 7.50 (t, $^3J(H,H) = 8.4$ Hz, 1H), 6.97 (m, 4H); MS (MALDI-TOF): *m*/*z*: 284 [$M+1$]$^+$; UV/Vis (CH_2Cl_2): λ_{max} (lg ε) = 516 (3.68), 480 (3.88), 450 (3.77), 425 (3.55), 376 (3.62), 356 (3.29), 271 (4.65), 261 nm (4.68); elemental analysis calcd (%) for $C_{19}H_9NO_2$: C 80.55, H 3.18, N 4.94; found C 80.28, H 3.04, N 5.05.

X-ray crystallography: Crystallographic data (excluding structure factors) for the structures reported in this paper have been deposited with the Cambridge Crystallographic Data Centre as supplementary publication nos. CCDC-148689 – 148694. Copies of the data can be obtained free of charge on application to the CCDC, 12 Union Road, Cambridge CB2 1EZ, U.K. (fax: (+44) 1223-336-033; e-mail: deposit@ccdc.cam.ac.uk). See Table 2 for general crystallographic details. Crystals of sufficient quality for X-ray crystallography were drawn directly from the respective mother liquors (**2b-PF_6** and **2d-PF_6** from methanol; **4b-BF_4**, **4c-BF_4**, and **6e-BF_4** from acetonitrile; and **8** from 1,2-dichlorobenzene). They were then coated with a thin layer of oil, mounted on glass needles with grease, and quickly transferred to the cold nitrogen stream of the diffractometer. All data were collected on a Siemens SMART Platform diffractometer with a CCD area-sensitive detector with $Mo_{K\alpha}$ radiation at 120(2) K. Absorption corrections were made for all the compounds by using SADABS.[45] Direct methods for the structure solution and full-matrix least-squares refinements were used for all the compounds with anisotropic temperature factors for all non-hydrogen atoms unless otherwise stated. Hydrogen atoms were included in calculated positions for all the compounds. The programs used were SMART, SAINT from Siemens,[46, 47] and SHELX-97.[48] All structures were checked for overlooked symmetry by using MISSYM and for voids by using PLATON.[49] Compounds **2b-PF_6**, **2d-PF_6**, **6e-BF_4**, and **8** crystallized with no associated solvent molecules, whereas compounds **4b-BF_4** and **4c-BF_4** crystallized with solvent molecules. The following details pertain to the treatment of the individual data sets, in particular with respect to modeling disorder. While **2b-PF_6** posed no problems, two molecules were found to be present in the asymmetric unit of **2d-PF_6**. Attempts were made to solve the

Table 2. Crystallographic data for compounds **2b-PF$_6$**, **2d-PF$_6$**, **4b-BF$_4$**, **4c-BF$_4$**, **6e-BF$_4$**, and **8**.

Compound	**2b-PF$_6$**	**2d-PF$_6$**	**4b-BF$_4$**	**4c-BF$_4$**	**6e-BF$_4$**	**8**
formula	$C_{26}H_{28}O_4NPF_6$	$C_{30}H_{28}O_4NPF_6$	$C_{58}H_{63}N_7BF_4$	$C_{45}H_{63}N_4BF_4$	$C_{25}H_{14}O_2NBF_4$	$C_{19}H_9O_2N$
M_r	563.46	611.50	1031.78	746.80	447.18	283.27
crystal system	monoclinic	triclinic	trigonal	triclinic	monoclinic	monoclinic
space group	$P2_1/c$	$P\bar{1}$	$R3$	$P\bar{1}$	$P2_1/n$	$C2/c$
Z	4	4	3	2	4	4
a [Å]	9.4760(15)	14.3212(4)	12.8285(11)	11.9581(8)	8.8267(10)	16.874(3)
b [Å]	14.130(3)	14.5140(4)	12.8285(11)	12.3668(9)	14.8644(16)	10.404(2)
c [Å]	19.419(4)	15.4376(4)	26.324(3)	15.8059(11)	14.6936(16)	7.2050(14)
α [°]	90	82.0050(10)	90	71.6540(10)	90	90
β [°]	103.447(7)	63.89	90	79.6370(10)	104.284(2)	110.61(3)
γ [°]	90	77.3130(10)	120	64.5430(10)	90	90
V [Å^3]	2528.8(9)	2807.72(13)	3751.8(6)	2000.5(2)	1868.3(4)	1183.9(4)
ρ [g cm^{-3}]	1.480	1.447	1.370	1.240	1.590	1.589
crystal size [mm]	$0.75 \times 0.45 \times 0.45$	$0.75 \times 0.63 \times 0.13$	$0.20 \times 0.20 \times 0.20$	$0.45 \times 0.3 \times 0.3$	$0.50 \times 0.25 \times 0.13$	$0.33 \times 0.04 \times 0.04$
μ [cm^{-1}]	0.187	0.175	0.101	0.085	0.127	0.104
reflections measured	26419	29754	16063	21870	23599	6078
unique reflections [$I > 2\sigma(I)$]	4407	9605	2332	5423	1215	701
R_{int}	0.0228	0.0209	0.0659	0.0244	0.2452	0.0689
$R(F)/R_w(F^2)$ all data	0.0356/0.0957	0.0572/0.1586	0.0960/0.3253	0.0690/0.2276	0.0738/0.1763	0.0519/0.1609

structure in a higher symmetry to avoid this;however, this was not possible and the difference between the two molecules in the asymmetric unit is evident from both the placement of the anions and the conformation of the benzyl group. The disorder was found to be quite pronounced in compounds **4b-BF$_4$** and **4c-BF$_4$**. Both were found to crystallize with acetonitrile solvent molecules. In **4b-BF$_4$**, the acetonitrile molecules were found between two anions and close to a threefold symmetry axis. This was modeled by neglecting the crystallographic symmetry, but setting the site occupation factor (sof) to 0.33333, thus giving a total of one acetonitrile solvent molecule at each site. Attempts were made to refine this model with respect to the sof. However, as the disorder is difficult to model, this gave rise to a higher sof than could be expected based on the NMR spectra of newly harvested crystals, which suggested the presence of one acetonitrile solvent molecule for every two $TATA^+$ molecules; the sof was therefore fixed at 0.33333. The thermal ellipsoids for the individual atoms of the acetonitrile solvent molecule were quite large. Several attempts to improve this were unsuccessful, and we chose to accept these large ellipsoids. Attempts were made to solve the structure in $R\bar{3}$, but this failed. In the structure of **4c-BF$_4$**, the disordered acetonitrile molecules were modeled as two mutually exclusive groups and were refined with respect to the sofs, which were found to be 0.457 and 0.543. Seven of the carbon atoms of one of the *n*-octyl groups were found to be disordered; again, this was modeled as two mutually exclusive groups and refined with respect to the sofs, which were found to be 0.238 and 0.762. Some atoms of the disordered *n*-octyl groups showed a tendency to become nonpositive definite (NPD) during the refinements; these were subjected to a soft constraint to make them approach isotropic behavior and to prevent them from becoming NPD. For compounds **2d-PF$_6$**, **4b-BF$_4$**, and **4c-BF$_4$**, the max/min residual electron densities were considerable: 1.526/ − 1.019, 1.341/ − 0.835, and 1.009/ − 0.639 (e/Å^3), respectively. For all the compounds, these peaks were found in the vicinity of the fluorine atoms of the anions, thus suggesting some disorder. In both cases, we attempted to apply a split model taking this disorder into account. No improvement was observed in terms of the *R* factor, hence the model presented here was chosen with acceptance of the residual electron density. In spite of the relatively poor data quality and the rather large *R* factor for compound **4b-BF$_4$**, we could unambiguously determine the connectivity, molecular conformation, packing pattern, and the spatial relationship between neighboring molecules.

Determination of pK_{R+} values: DMSO was purified by distillation from CaH_2 at 10 mmHg argon pressure. Dissolved oxygen was removed from all stock solutions by purging with argon. Concentrated stock solutions of the carbenium salts **4a**, **6a**, and **7b** in DMSO were prepared from the PF_6 salts and injected through a septum into the absorption cell, which contained a known volume of DMSO/water/Me_4NOH solution. After each measurement, a few μL of aqueous HCl was added to check the reversibility. By using this method, the entire procedure (injection of the dye, mixing, recording of spectra, and acidification) could be accomplished within a few minutes, or even less when the absorbance was monitored at only one wavelength.

The equilibrium distributions between cations and carbinols were obtained from the relative concentrations, which were determined by UV/Vis spectrophotometry at wavelengths at which only the cationic compounds absorb. The pK_{R+} values were derived from linear fits to plots of log([ROH]/[R^+]) versus $C\_$ for each solution. The $C\_$ values for the individual solutions (of known compositions) were evaluated from a new improved representation, obtained by modifying a seventh-order fit to the $H\_$ data (10 to 98.3 mol% DMSO) given in the article of Dolman and Stewart.[50] The $C\_$ function was obtained by multiplying the coefficients in Equation (1) by 1.31 and assigning the constant term α such a value that the new function $C\_$ gives a value of 13.51 when $X = 12.1$ (see ref. [8]). The expressions used to represent $H\_$ and $C\_$ are given by:

$$Y\_(X) = \alpha + \beta 1\,X + \beta 2\,X^2 + \beta 3\,X^3 + \beta 4\,X^4 + \beta 5\,X^5 + \beta 6\,X^6 + \beta 7\,X^7 \quad (1)$$

in which $Y\_$ is $H\_$ or $C\_$ and X is the mol% of DMSO in the DMSO/water mixtures with 0.011M Me_4NOH. The constants α and $\beta 1 - \beta 7$ are given in Table 3.

Table 3. Coefficients to the seventh-order polynomiums [Eq. (1)] used to simulate $C\_$ and $H\_$.

	$H\_$	$C\_$
α	9.62482118	8.48103
$\beta 1$	0.59460716	0.77893538
$\beta 2$	− 0.03624451	− 0.04748031
$\beta 3$	0.00144569	0.00189385
$\beta 4$	− 3.33937E − 5	− 4.37458E − 5
$\beta 5$	4.42876E − 7	5.80168E − 7
$\beta 6$	− 3.11739E − 9	− 4.08378E − 9
$\beta 7$	9.01042E − 12	1.18037E − 11

Acknowledgement

We thank Dr. Armin R. Ofila, Institute of Organic Chemistry, University of Munich, for his helpful comments on the $C\_$ acidity function, and Dr. Mikkel Jørgensen, Risø National Laboratories, for fruitful discussions.

  0947-6539/01/0708-1782 $ 17.50+.50/0

[1] *The Chemistry and Applications of Dyes* (Eds.: D. R. Waring, G. Hallas), Plenum, New York, **1990**.
[2] K. H. Drexhage, in *Dye Lasers* (Ed.: F. P. Schäfer), Springer, **1990**, pp. 155–200.
[3] R. P. Haugland, *Handbook of Fluorescent Probes and Research Chemicals*, 6th ed., Molecular Probes, Eugene, OR, **1996**.
[4] H. H. Freeman, in *Carbonium Ions* (Eds.: G. A. Olah, P. von R. Schleyer), Wiley-Interscience, New York, **1973**.
[5] E. M. Arnett, R. A. Flowers II, in *Stable Carbocation Chemistry* (Eds.: G. K. Surya Prakash, P. v. R. Schleyer), Wiley, **1997**, pp. 265–296.
[6] K. Komatsu, H. Akamatsu, Y. Jinbu, K. Okamoto, *J. Am. Chem. Soc.* **1988**, *110*, 633–634.
[7] S. Ito, S. Kikuchi, N. Morita, T. Asao, *J. Org. Chem.* **1999**, *64* , 5815–5821.
[8] B. W. Laursen, F. C. Krebs, M. F. Nielsen, K. Bechgaard, J. B. Christensen, N. Harrit, *J. Am. Chem. Soc.* **1998**, *120*, 12255–12263.
[9] P. Huszthy, K. Lempert, G. Simig, J. Tamás, *J. Chem. Soc. Perkin Trans. 2* **1982**, 1671–1674.
[10] P. Huszthy, K. Lempert, G. Simig, K. Vékey, *J. Chem. Soc. Perkin Trans. 1* **1982**, 3021–3025.
[11] M. Wada, T. Watanabe, S. Natsume, H. Mishima, K. Kirishima, T. Erabi, *Bull. Chem. Soc. Jpn.* **1995**, *68*, 3233–3240.
[12] L. Teruel, L. Viadel, J. Carilla, L. Fajari, E. Brillas, J. Sane, J. Rius, L. Juliá, *J. Org. Chem.* **1996**, *61*, 6063–6066.
[13] J. C. Martin, R. G. Smith, *J. Am. Chem. Soc.* **1964**, *86*, 2252–2256.
[14] F. A. Carey, H. S. Tremper, *J. Am. Chem. Soc.* **1968**, *90*, 2578–2583.
[15] M. R. Feldman, W. C. Flythe, *J. Org. Chem.* **1978**, *43*, 2596–2600.
[16] W. T. Bowie, M. R. Feldman, *J. Am. Chem. Soc.* **1977**, *99*, 4721–4726.
[17] R. J. Smith, R. M. Pagni, *J. Am. Chem. Soc.* **1979**, *101*, 4769–4770.
[18] R. J. Smith, T. M. Miller, R. M. Pagni, *J. Org. Chem.* **1982**, *47*, 4181–4188.
[19] M. J. Sabacky, C. S. Johnson, R. G. Smith, H. S. Gutowsky, J. C. Martin, *J. Am. Chem. Soc.* **1967**, *89*, 2054–2058.
[20] E. Müller, A. Moosmayer, A. Rieker, K. Scheffler, *Tetrahedron Lett.* **1967**, *39*, 3877–3880.
[21] H. Kessler, A. Moosmayer, A. Rieker, *Tetrahedron* **1969**, *25*, 287–293.
[22] F. A. Neugebauer, D. Hellwinkel, G. Aulmich, *Tetrahedron Lett.* **1978**, *49*, 4871–4874.
[23] M. Lofthagen, J. S. Siegel, *J. Org. Chem.* **1995**, *60*, 2885–2890.
[24] M. Lofthagen, J. S. Siegel, R. Chadha, *J. Am. Chem. Soc.* **1991**, *113*, 8785–8790.
[25] M. Lofthagen, J. S. Siegel, R. V. Clark, K. K. Baldridge, *J. Org. Chem.* **1992**, *57*, 61–69.
[26] G. Allison, R. J. Bushby, J.-L. Paillaud, *J. Am. Chem. Soc.* **1993**, *115*, 2062–2064.
[27] G. Allison, R. J. Bushby, J.-L. Paillaud, M. Thornton-Pett, *J. Chem. Soc. Perkin Trans. 1* **1995**, 385–390.
[28] J. Reynisson, Ph.D. Thesis, **2000**, Risø National Laboratory, Roskilde (Denmark).
[29] F. C. Krebs, P. S. Larsen, J. Larsen, C. S. Jacobsen, C. Boutton, N. Thorup, *J. Am. Chem. Soc.* **1997**, *119*, 1208–1216.
[30] G. K. H. Madsen, F. C. Krebs, B. Lebech, F. K. Larsen, *Chem. Eur. J.* **2000**, *6*, 1797–1804.
[31] A. Faldt, F. C. Krebs, N. Thorup, *J. Chem. Soc. Perkin Trans. 2* **1997**, 2219–2227.
[32] F. C. Krebs, B. W. Laursen, I. Johannsen, A. Faldt, K. Bechgaard, C. S. Jacobsen, N. Thorup, K. Boubekeur, *Acta. Crystallogr. Sect. B* **1999**, *55*, 410–423.
[33] J. W. Bunting, W. G. Meathrel, *Can. J. Chem.* **1973**, *51*, 1965–1972.
[34] B. W. Laursen, F. C. Krebs, *Angew. Chem.* **2000**, *112*, 3577–3579; *Angew. Chem. Int. Ed.* **2000**, *39*, 3432–3434.
[35] P. Huszthy, K. Lempert, G. Simig, *J. Chem. Soc. Perkin Trans. 2* **1985**, 1351–1354.
[36] W. Schroth, W. Dölling, in *Methoden Org. Chem. (Houben-Weyl)*, *4th ed. 1952–*, Vol. E7b, **1992**, pp. 964–1004.
[37] J. Reynisson, G. Balakrishnan, R. Wilbrandt, N. Harrit, *J. Mol. Struct.* **2000**, *520*, 63–67.
[38] The crystal structure of 2,6,10-tris(*N*-pyrrolidinyl)-4,8,12-trioxatriangulenium hexafluorophosphate is reported in ref. [8]. The structure of the tetraphenylborate salt of $(Et_2N)_3$-TOTA$^+$, which has recently been solved, shows a similar packing pattern (unpublished result from this laboratory).
[39] J. Griffiths, *Colour and Constitution of Organic Molecules*, Academic Press, **1976**.
[40] A. Samanta, K. R. Gopidas, P. K. Das, *J. Phys. Chem.* **1993**, *97*, 1583–1588.
[41] A. Anne, S. Fraoua, P. Hapiot, J. Moiroux, J. M. Sevéant, *J. Am. Chem. Soc.* **1995**, *117*, 7412–7421.
[42] N. C. Deno, J. J. Jaruzelski, A. Schriesheim, *J. Am. Chem. Soc.* **1955**, *77*, 3044–3051.
[43] For the H_- function evaluated by Dolman and Stewart for deprotonation of anilines and diphenylamines in the DMSO/water/tetramethylammonium hydroxide system, see ref. [50].
[44] See: ref. [4], and references therein.
[45] Empirical absorption program (SADABS) written by G. Sheldrick for the Siemens SMART platform.
[46] G. M. Sheldrick, *SHELXTL-95*, Siemens Analytical X-ray Instruments, Madison, Wisconsin (USA), **1995**.
[47] *SMART* and *SAINT*, *Area-Detector Control and Integration Software*, Siemens Analytical X-ray Instruments Inc., Madison, Wisconsin (USA), **1995**.
[48] G. M. Sheldrick, *SHELX-97, Program for Structure Solution and Refinement*, University of Göttingen **1997**.
[49] A. L. Spek, *Acta Crysallogr. Sect. A* **1990**, *46*, C-34.
[50] D. Dolman, R. Stewart, *Can. J. Chem.* **1967**, *45*, 911–924.

Received: September 4, 2000 [F2707]